AIAA JOURNAL
Vol. 39, No. 9, September 2001

Technical Notes

TECHNICAL NOTES are short manuscripts describing new developments or important results of a preliminary nature. These Notes cannot exceed six manuscript pages and three figures; a page of text may be substituted for a figure and vice versa. After informal review by the editors, they may be published within a few months of the date of receipt. Style requirements are the same as for regular contributions (see inside back cover).

Swept Thin Wings in Unsteady Sonic Flow

Paulo A. O. Soviero* and Guilherme A. V. César†
Instituto Tecnológico de Aeronáutica,
12228-900 São José dos Campos, Brazil

Introduction

THE linearized unsteady potential equation in the transonic range as proposed by Landahl[1] is consistent because it provides the realistic limit to the wave equation usually adopted in linearized unsteady subsonic and supersonic flow over lifting surfaces. In fact, acoustical theory introduces oscillations that are not in accordance with physical reality for flows around Mach number one.

The present investigation proposes a numerical method to solve the transonic unsteady linearized equation that allows the accurate analysis of swept thin wings in harmonic oscillatory motion. Early attempts to solve this problem in a satisfactory general way were made by Runyan and Woolston,[2] who extended the subsonic kernel function method based on the acceleration potential formulation to the Mach one limit. However, this depends on suitable loading functions. A complete numerical scheme is provided by the sonic box scheme from Rodemich and Andrew[3] that incorporates discrete rectangular panels of constant doublet density of velocity potential. If swept wings are to be calculated, a discretization based on rectangular small boxes brings out convergence concerns. The slow convergence rate as a function of the number of boxes over the wing and spurious disturbances of solutions, as reported in Ref. 4, for delta and cropped-delta wings, can be caused by the crude approximations of the wing planform by the box arrays. This is especially true along swept edges and tips or complicated modes of deformation such as might be required for flutter analysis.

The new proposed method of solution presented here is based on results from Ref. 5, where an analytical expression is derived for the rectangular box downwash. This technique allows the obtaining of an expression applicable for quadrilateral boxes with only two parallel edges in the chordwise direction, which fits exactly all swept edges and allows suitable discretization of realistic wings.

Integral Equation

The integral equation to be solved has been already discussed in Ref. 5 and relates the potential jump amplitude $\delta\phi$ across the lifting surface at a point (x_0, y_0) and the downwash amplitude w at a point (x, y), that is,

$$w(x, y) = \frac{1}{4\pi} \iint \delta\phi \frac{ik}{(x - x_0)^2} \exp\left[-\frac{ik(y - y_0)^2}{2(x - x_0)}\right] \mathrm{d}x_0 \, \mathrm{d}y_0 \tag{1}$$

The configuration is planar and placed in an uniform sonic freestream of unitary velocity. The oscillation proceeds at a reduced frequency k, based on the the root semichord of the wing.

The integration of Eq. (1), which represents a doublet distribution of density $\delta\phi$ inducing a normal velocity on the downwash point (x, y), must be performed over an area of the wing, which is ahead of (x, y). It is also important to keep in mind that along y_0 the interpretation of the integral sign is usual, but along x_0 the interpretation is according to the finite-part sense.

The boundary condition for wings with sonic trailing edge is written as

$$w(x, y) = \exp(ikx/2)\left(\frac{\partial h}{\partial x} + ikh\right) \tag{2}$$

where $h(x, y)$ represents the wing surface nondimensional vertical displacement. For further details concerning the mathematical model, the reader is referred to Ref. 5.

Numerical Method

Solutions of integral Eq. (1) for wings with sonic trailing edge are obtained by discretization of the planform through the use of small quadrilateral elements. Over each panel uniform density doublets are distributed from the swept leading edge of the panel down to the trailing edge of the wing. This type of discretization is similar to that employed in the classical vortex lattice method. A general view of the discretized wing and elemental panel with superimposed uniform density doublets represented by dashed lines is also shown in Fig. 1a.

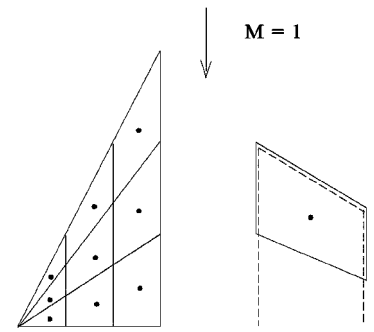

Fig. 1a Wing discretization and elemental panel.

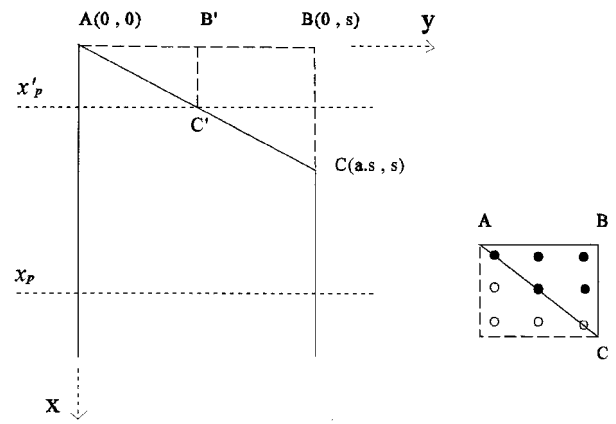

Fig. 1b Local panel reference frame for analytical and numerical integrations on rectangular domain.

Received 9 December 2000; revision received 10 April 2001; accepted for publication 25 May 2001.

*Professor, Aeronautical Engineering Division; soviero@aer.ita.br. Member AIAA.

†Graduate Student and Test Engineer, Aeronautical Engineering Division; vargas@iae.cta.br.

The influence coefficients are obtained, for points x_p midway between leading and trailing edges of the panel, from the expression already deduced in Ref. 5 for the rectangular panel whose leading edge spans from A to B (Fig. 1b) and reads

$$F(x_p, y_p) = -\frac{1}{2\pi}\left[\frac{\exp(-\lambda_1^2)}{s - y_p} + \frac{\exp(-\lambda_2^2)}{s}\right] + \frac{1}{2}\sqrt{\frac{ik}{2\pi x_p}}\,[\mathrm{erf}(\lambda_1) - \mathrm{erf}(\lambda_2)] \tag{3}$$

where

$$\lambda_1 = (y_p - s)\sqrt{ik/2x_p}, \qquad \lambda_2 = y_p\sqrt{ik/2x_p} \tag{3a}$$

for $x_p > 0$ and zero otherwise. In the spanwise direction y_p is also midway along the panel span.

The final formula for the influence coefficients of the panel with sweep leading edge is obtained from the expression in Eq. (3) minus the normal wash induced by the triangular element A, B, C, A. Because it was not possible to obtain a complete analytical integration of Eq. (1), for unitary $\delta\phi$ a numerical double integration is performed. The numerical scheme of integration employed is equivalent to a Gauss–Legendre numerical quadrature with nine points spread over the rectangle defined as in Fig. 1b; the remainder is of order max $\{s^6, (a.s)^6\}$ as can be deduced from Ref. 6.

To assess the numerical convergence characteristics of the proposed numerical integration, consider the triangular domain A, B, C, A and unitary $\delta\phi$. After integrating Eq. (1) in y_0, one obtains

$$F(x_p, y_p) = \frac{1}{4}\sqrt{\frac{ik}{2\pi}}\int_0^{as} \frac{\mathrm{erf}(\lambda_3) - \mathrm{erf}(\lambda_4)}{(x_p - x_0)^{3/2}}\,\mathrm{d}x_0 \tag{4}$$

where

$$\lambda_3 = (y_p - ax_0)\sqrt{\frac{ik}{2(x_p - x_0)}}, \qquad \lambda_4 = (y_p - s)\sqrt{\frac{ik}{2(x_p - x_0)}} \tag{4a}$$

and a is the tangent of the leading-edge sweep angle of the panel considered.

If x_p is greater than $a.s$, Eq. (4) admits a regular integrand, and the numerical integration of Eq. (1) for the purpose of determining the influence coefficients is straighforward. For the limiting case when x_p equal $a.s$, if we assume that k has a small negative imaginary part Eq. (4) becomes also regular because then the integrand goes to zero as x_0 tends to x_p. For k strictly real Eq. (4) is not integrable, neither its integral defined in the finite-part sense. From the point of view of the numerical quadrature just discussed, disregarding the point closer to C (see Fig. 1b) is equivalent to assuming that k has a small negative part. The same procedure is also applicable for a point x'_p between A and B in the streamwise direction (see again Fig. 1b) where for this case one must take B′ and C′ instead of B and C.

Results and Discussion

Numerical calculation for a triangular wing of aspect ratio 1.5 is performed, and the results are compared with earlier publications by Landahl,[1] Rodemich and Andrew,[3] and Davies.[7] Landahl and Davies worked anlytically, whereas Rodemich and Andrew employed rectangular panels in their numerical procedure.

Figure 2 shows unsteady results for the triangular wing in heaving motion. Lift coefficient amplitude per reduced frequency and phase angle compare fairly well with the third-order solution of Landahl.[1] The vertical scales of Fig. 2 have been expanded in the portion of interest. All analytical approaches, just like the present calculation, tend to the correct value for the zero reduced frequency as predicted by the slender wing theory. Davies results compare faily well with Landahl's because both final formulas come from the same mathematical model. Their first-order terms are equal, and the differences come from the way they evaluate second and third-order ones.[1,7] For the present calculations a grid of 216 panels (24×9 points along the chord and semispan, respectively) was used for the half-wing. Results for a grid of 384 panels (32×12 points) are also shown

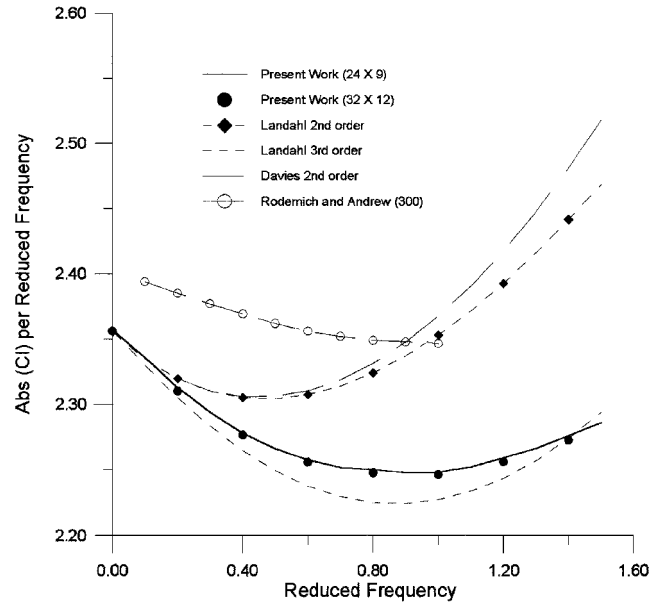

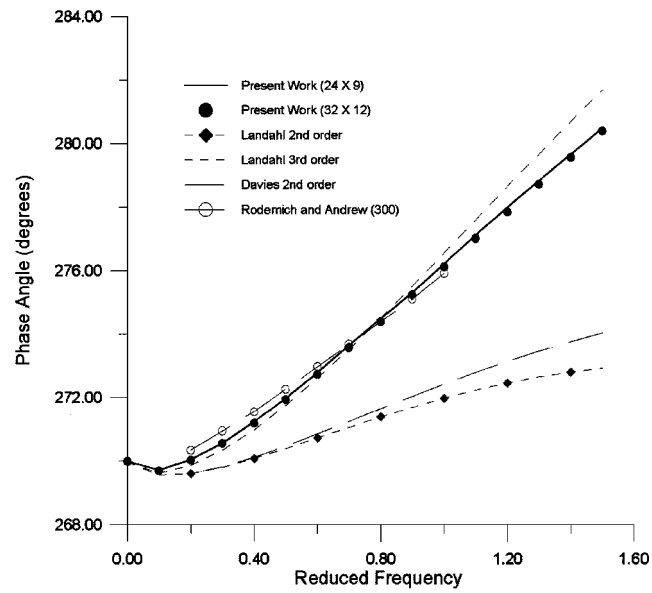

Fig. 2 Triangular wing of aspect ratio 1.5 in heaving motion: reduced frequency based on wing root chord.

in order to illustrate the convergence behavior of the present proposed numerical method. For both calculations the limit values for zero reduced frequency converge to the analytical one obtained from slender body theory ($\pi/2 \cdot$ aspect ratio). The differences in results for both discretizations for all reduced frequencies studied amount to less than 0.20% of the exact steady flow value for the worst case. Because the proposed numerical scheme is a constant velocity potential method, the control points location employed are equivalent to the $\frac{1}{4}$–$\frac{3}{4}$ chord rule as is usual in all vortex lattice method versions. Observation of Fig. 2 also shows that the results of Rodemich and Andrew[3] are good as far as phase angle is concerned, although the lift coefficient amplitude per reduced frequency is consistently overpredicted.

Conclusions

The present work presents a numerical method to solve the linearized unsteady sonic equation over lifting surfaces by means of a panel discretization that fits exactly the wing planform. For most part of the calculations, the overall agreement with earlier results is very good. Eventual discrepancies concerning low reduced frequencies behavior of analytical formulas would deserve better analysis.

Acknowledgment

This work was partially supported by the Brazilian Council for Scientific and Technological Research (CNPq) under Grant 300.682/93-0.

References

[1]Landahl, M. T., *Unsteady Transonic Flow*, Pergamon, Oxford, 1961, pp. 7–21.

[2]Runyan, H. L., and Woolston, D. S., "Method for Calculating the Aerodynamic Loadings on Oscillating Finite Wing in Subsonic and Sonic Flow," NACA Rept. 1322, 1957.

[3]Rodemich, E. R., and Andrew, L. V., "Unsteady Aerodynamics for Advanced Configurations, Part II—A Transonic Box Method for Planar Lifting Surfaces," U. S. Air Force Research Lab., FDL-TRD-64-152, Pt. II, Wright–Patterson AFB, OH, May 1965.

[4]Yates, E. C., Jr., "Unsteady Transonic Flow—Introduction, Current Trends, Applications," *Computational Methods in Potential Aerodynamics*, Springer-Verlag, Berlin, 1985, pp. 502–568.

[5]Soviero, P. A. O., and Pinto, F. H. L., "Unsteady Lifting Surface Theory in Sonic Flow: The Problem Revisited," *AIAA Journal*, Vol. 38, No. 5, 2000, pp. 931–933.

[6]Abramowitz, M., and Stegun, I. A. (eds.), *Handbook of Mathematical Functions, with Formulas, Graphs, and Mathematical Tables*, 9th ed., Dover, New York, 1970, p. 892.

[7]Davies, D. E., "Three Dimensional Sonic Flow Theory," *AGARD Manual on Aeroelasticity*, Pt. 2, 1960, Chap. 4, pp. 74–76.

A. Plotkin
Associate Editor

Effects of Changing Aspect Ratio Through a Wind-Tunnel Contraction

John Callan* and Ivan Marusic†
University of Minnesota, Minneapolis, Minnesota 55455

I. Introduction

ALMOST all high-quality wind tunnels use a contraction section to accelerate the flow into the working section. Obviously, the design of the contraction shape is crucial for producing the desired low-turbulence, uniform exit stream. Most present-day design rules are based on theoretical and computational studies that consider inviscid irrotational flow, and perhaps the best known of these is the study of Morel.[1] Morel analyzed contractions with an axisymmetric geometry and produced a series of design charts, giving the designer a tool for optimizing contraction length, contraction ratio, and curve shape based on the criteria of the possibility of separation in the contraction, along with the exit flow nonuniformity. It was concluded that the best contraction shapes were curves consisting of two matched cubic arcs whose match point is a varying parameter.

Although the majority of previous studies have concentrated on axisymmetric contractions, most wind-tunnel contractions are not axisymmetric but rather are three dimensional with rectangular cross-section. In this case an important parameter is the aspect ratio, denoted by AR and defined as the width/height at a given position in the contraction. One numerical study that has considered the design of three-dimensional contractions is that of Su,[2] who computed solutions to the three-dimensional Laplace equation. Based on the Morel criteria,[1] Su showed[2] that three-dimensional contractions exhibit poorer qualities, in terms of the possibility of flow separation and exit flow nonuniformity, than axisymmetric contractions with similar geometric properties (contraction ratio, etc.). The explanation given is that the presence of corners in the three-dimensional case produces greater velocity extrema than in the axisymmetric case. A feature that is present in three-dimensional contractions and not in axisymmetric ones is the effect of crossflow in the contraction. Su showed that the crossflow is induced due to the transverse pressure gradient existing in the contraction. This pressure gradient exists because of greater local velocity extrema at the corners relative to the centerline velocities on the walls on the planes of symmetry. A crossflow parameter was considered that showed the relative strengths of the crossflow effect for different contraction designs. No conjecture was attempted, however, on the effect of this crossflow on the flow quality at the exit, specifically on its effect on boundary-layer development. Su performed a parametric study by varying the important design parameters and studying their effect on the criteria set out by Morel.[1]

These previous studies, and others,[3,4] have focused on the numerical solution to the flow in the contraction for use as a tool for predicting the flow quality at exit. One study, that of Tulapurkara and Bhalla,[5] performed an experimental analysis of the flow in a contraction, in an attempt to verify Morel's predictions.[1] No studies, however, have focused on the actual flow in the working section at the exit of a contraction and the effect of changing the geometric parameters of the contraction on it. Furthermore, no previous studies have looked at the role that changing the AR through the length of the contraction has on the corner boundary layers. In the absence of any studies, designers have generally relied on rules of thumb to guide them. One of these is the so-called pyramid rule (A. E. Perry, private communication, 1997), which states that AR should be held constant throughout the contraction to minimize the growth of the corner boundary-layer vortices into the working section of the wind tunnel. This rule conflicts with the conclusion of Su[2] that changing AR can be advantageous when separation criteria are considered. However, because Su's study is based on solutions to potential flow, no rational comparison can be made. Maintaining a constant AR through the length of the contraction can often be impractical because of space constraints and also becomes a trade-off between varying other important parameters such as a higher contraction ratio, for example.

In this Note, we address the issue of changing the AR through a contraction by keeping inlet AR fixed at 1 and varying exit AR, while keeping the shape, contraction ratio, and length fixed. In this way, we can perform a parametric study of changing AR effects while keeping all other important parameters constant.

II. Experimental Procedure

Four contractions were constructed and were fitted to an existing wind-tunnel facility, each with fixed values for the various geometric parameters, with the exception of exit AR. The values of the fixed parameters are given in Table 1. As indicated in Table 1, the length of the contraction is denoted as L, A_i and A are the cross-sectional areas of the inlet and exit of the contraction respectively, and D_i and D are the inlet and exit effective diameters, respectively, where $D = (4A/\pi)^{1/2}$. The shape of the contraction surfaces are matched cubic arcs (following Morel[1] and Su[2]), where x_m is the distance from the beginning of the contraction to the match point of the cubic curves. The exit AR variation is given in Table 2.

Full details of the design and construction of the contractions are given by Callan.[6] In all cases, a short working section was attached to the exit of the contraction. Streamwise velocity and turbulence intensity measurements were made with a single component hot wire, one effective exit diameter downstream of the contraction exit. Data were gathered across the plane with the wires oriented both parallel

Table 1 Fixed parameters in study

Parameter	Value
Inlet area A_i, mm^2	600×600
Contraction ratio A_i/A	8.72
Contraction length/inlet effective diameter L/D_i	1.0
Contraction length L, mm	685
Cubic match point x_m/L	0.6
Exit Reynolds number $Re = U_e D/\nu$	4.8×10^5

Received 24 October 2000; revision received 4 June 2001; accepted for publication 4 June 2001.

*Research Assistant, Department of Aerospace Engineering and Mechanics.

†Assistant Professor, Department of Aerospace Engineering and Mechanics. Member AIAA.